



Project 059(E) Moderate-fidelity Simulations for Efficient Modeling of Supersonic Aircraft Noise

The Pennsylvania State University

Project Lead Investigator

Philip Morris
Boeing/A.D. Welliver Professor Emeritus
Department of Aerospace Engineering
Pennsylvania State University
243 ECoRE Building
University Park, PA 16802
814-360-8681
pjm@psu.edu

University Participants

Pennsylvania State University (Penn State)

- P.I.s: Dr. Philip Morris (P.I.), Dr. Daning Huang (co-P.I.)
- FAA Award Number: 13-C-AJFE-GIT-070
- Period of Performance: January 1, 2025, to September 30, 2025
- Tasks:
 1. Coarse grid large eddy simulations (LES)
 2. Hybrid Reynolds-averaged Navier-Stokes (RANS) and acoustic analogy for noise predictions

Project Funding Level

The ASCENT Project 059E is funded at the following level: \$100,000 from Federal Aviation Administration (FAA) and \$100,000 in cost-sharing funding provided by Gulfstream Aerospace Corporation, a General Dynamics Company.

Investigation Team

Dr. Philip Morris (P.I.), All Tasks
Dr. Daning Huang (co-P.I.), All Tasks
Ms. Dana Mikkelsen (graduate student), All Tasks
Mr. Aravinth Sadagopan (graduate student), Computational fluid dynamics (CFD) tasks

Project Overview

The purpose of this project is to develop and assess efficient computational tools to simulate the flow and noise of civil supersonic aircraft engines.

The prediction of noise from supersonic jets, particularly when noise reduction devices are present, is a challenging computational task. Methods based on RANS solutions are relatively inexpensive to perform and provide satisfactory predictions of the average flow field, even for quite complicated geometries. The subsequent prediction of noise according to acoustic analogies is highly efficient but faces difficulties when the nozzle does not have simple axisymmetric geometry. Methods based on LESs provide considerably more information than those based on RANS methods about the unsteady flow and the noise generated. However, LESs are computationally expensive, particularly when the engine geometry is complex. This complexity is encountered in the case of nozzles with noise reduction devices, such as internal mixers. Noise predictions based on LES can be made quite efficiently by using the Ffowcs Williams and Hawkins (FW-H) acoustic analogy (Farassat & Succi, 1982; Ffowcs Williams & Hawkins, 1969), but long-time records are required to predict the noise radiated to far-field observers, thus adding additional expense to LES.



The approach in ASCENT Project 059E strikes a compromise between the accuracy and high computational cost of LES and the noise prediction limitations of RANS-based simulations. The RANS solution at the jet exit will be used as an initial condition for the external LES. This process will require the addition of some unsteady information based on linear instability modes. This approach will reduce the total computational cost because it removes much of the geometric complexity and the associated grid requirements for LES of the internal flow.

In addition, the LES-based predictions will be supplemented by more traditional acoustic analogy approaches based on RANS. As described below, the future research direction combines a RANS-based acoustic analogy approach for noise radiation to large angles to the jet downstream axis and a very coarse LES approach for noise radiation in the peak noise radiation direction.

If successful, ASCENT Project 059E will develop methods to predict the noise generated and radiated by civil supersonic aircraft engines. The developed tools should enable airframe and engine manufacturers to assess the noise impacts of engine design changes, and to determine whether the designs will meet current or anticipated noise certification requirements.

Major Accomplishments

The tasks for this project year included continued RANS simulations and LESs. The focus was on the Georgia Institute of Technology (Georgia Tech) dual-stream nozzle. LES simulations were performed at Gulfstream Aerospace, by using different grid resolutions to determine the flow resolution relative to different turbulent length scales. An acoustic analogy code was based on the Tam and Auriault (1999) model (Tam & Auriault, 1999) and integrated with output from the RANS simulations. Noise predictions with this method have been made for the Georgia Tech dual-stream nozzle and compared with measurements.

Task 1 – Coarse LES Simulations

Pennsylvania State University
Gulfstream Aerospace

Objectives

The goal of this task is to generate an LES using a coarse grid and then use the Ffowcs Williams-Hawkings acoustic analogy to predict the radiated noise. It is expected that the predicted noise radiation will only be reasonably accurate in the peak noise directions close to the jet downstream direction. As is noted below, trouble was found in generating the unsteady flow field prior to making noise predictions.

Research Approach

The case considered is described here. The nozzle exit is at 0.652336 m and diameter (D) is 0.0432 m. The complete nozzle is shown in Figure 1 for reference. The operating conditions are given in Table 1.

A steady-state RANS computation was performed for the nozzle configuration and grid shown in Figure 2. The mesh discretization involved 20 million finite volume (FV) cells with polyhedral cells and mesh adaptivity tailored to regions with high Mach number gradient. The objective was to resolve the shear layer at nozzle exit. The far field had cell size of 0.15 m and the nozzle wall had cells with size varying from 0.4 mm to 1 mm. A prism layer is specified on the nozzle wall to resolve the incoming boundary layer with thickness of 6 mm and 12 layers. The numerical scheme is detailed below. A stagnation inlet condition is specified for core and bypass inflow, and the far field is specified as freestream. The remainder of the surfaces are specified as wall with no-slip condition.

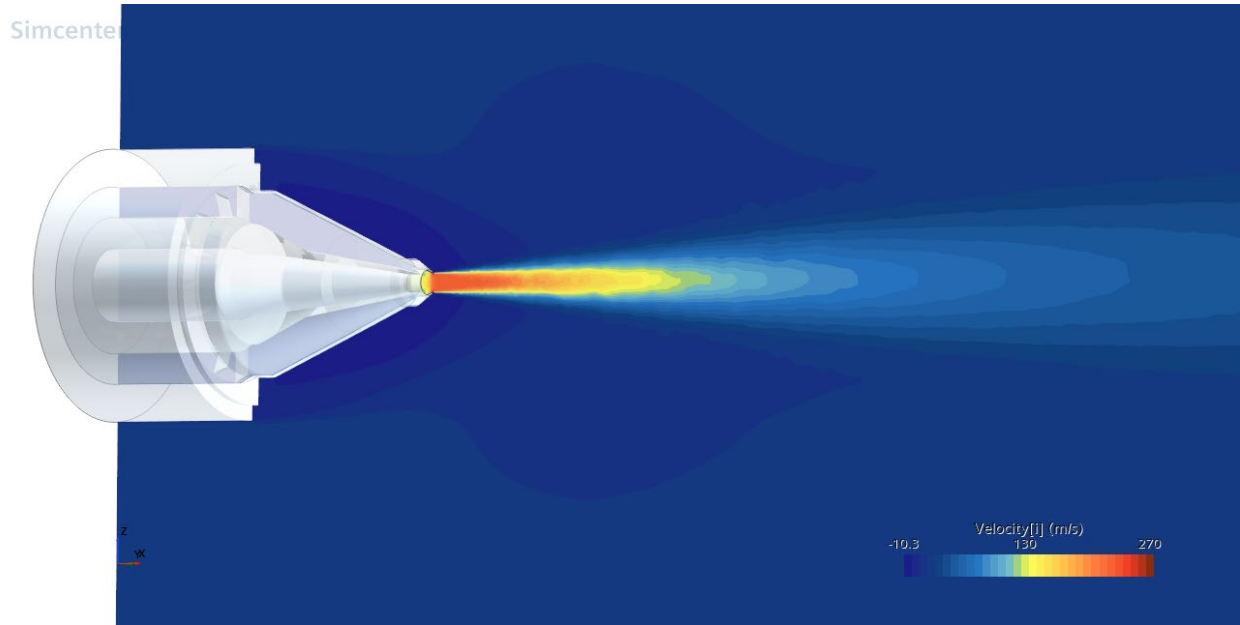


Figure 1. Geometry of jet nozzle exhaust in the present study. Velocity contour shown for NPR_1_39 case.

Table 1. Operating conditions for the dual stream nozzle.

Parameter	Core	Bypass
Nozzle pressure ratio, NPR	1.39	1.39
Nozzle temperature ratio, NTR	1	1
Total pressure, P_t	135219.98 Pa	135219.98 Pa
Total temperature, T_t	296.4433 K	296.4433 K
Jet Mach number, M	0.699	0.699
Velocity, U	230 m/s	230 m/s
	Freestream	
Reference pressure, P_{ref}	97547 Pa	
Reference temperature, T_{ref}	295.45 K	
Initial Temperature, T_i	5.0e-4	

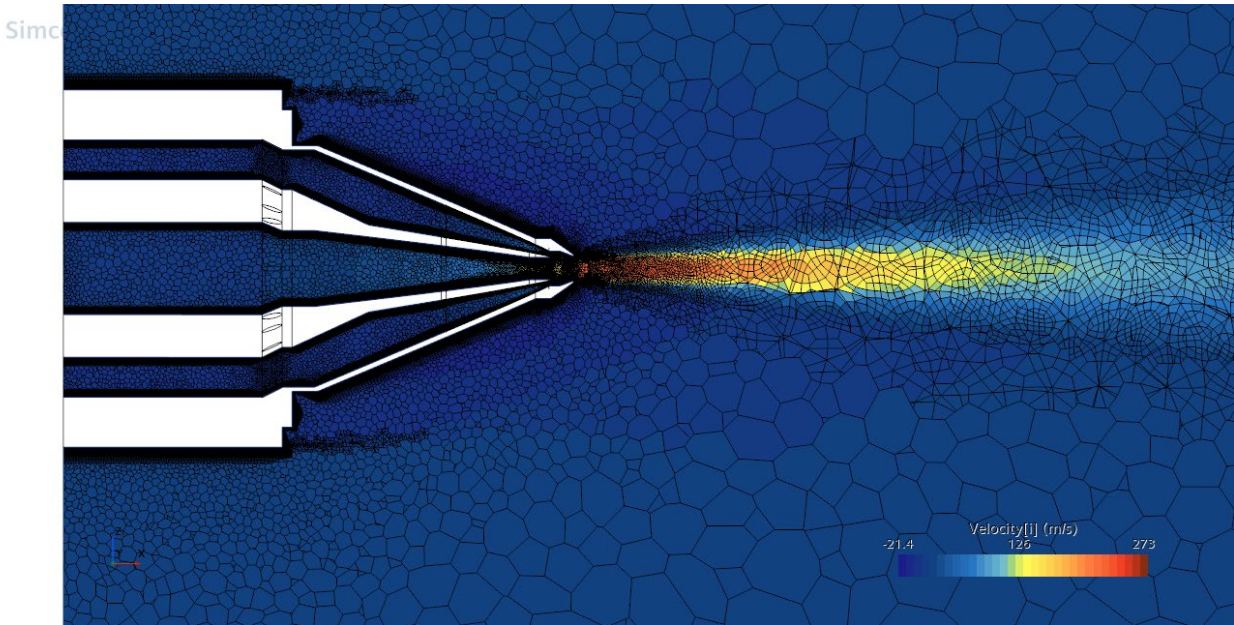


Figure 2. Jet nozzle configuration with the finite volume mesh. The Mach number contour corresponds to NPR_1_39 case.

Validation of the RANS with Experimental Results

The computational results were compared with the experimental particle imaging velocimetry measurements for the downstream section. Figure 3 compares the non-dimensionalized axial velocity with the experimental data at the centerline and lip line. It is observed that the predicted axial velocity at the core decreases at a faster rate than the experiment whereas it reasonably matches at the lip line. Figure 4 compares the axial velocity profiles downstream of the nozzle at different axial locations and the RANS predictions match with experimental data. Figure 5 provides a comparison of turbulent kinetic energy (left) and axial velocity (right) contours with the experiment.

A second order upwind scheme with AUSM+ inviscid flux was used for the RANS simulation. Diffusion is enabled at flow boundaries. To model turbulence, the $k - \omega$ shear stress transport (SST) (Menter) model was implemented with the assumption of ideal gas.

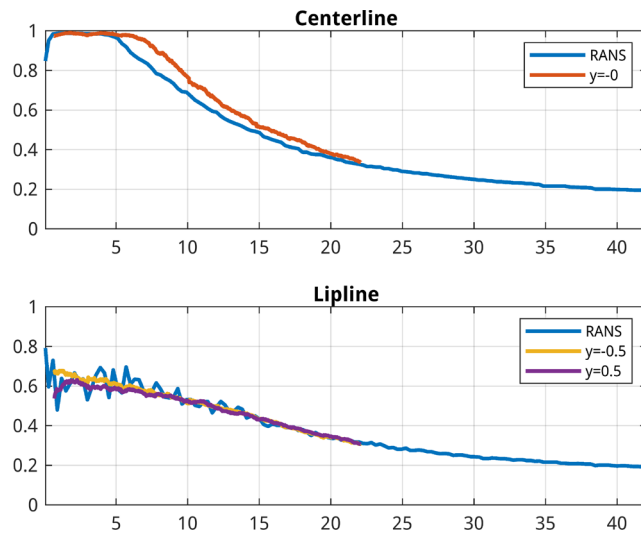


Figure 3. Comparison of non-dimensional axial velocity with the experimental data at centerline and lip line.

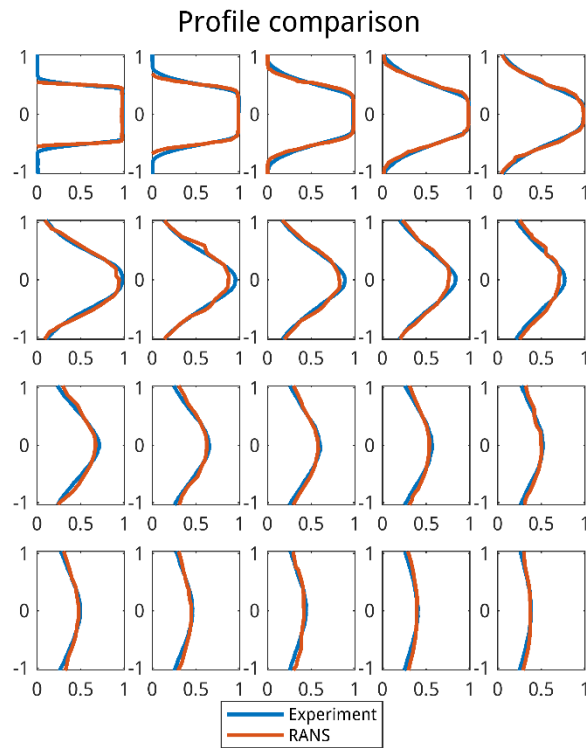


Figure 4. Comparison of axial velocity profiles downstream of the nozzle exit. $x/D = 0$ to 20 from top left to bottom right.

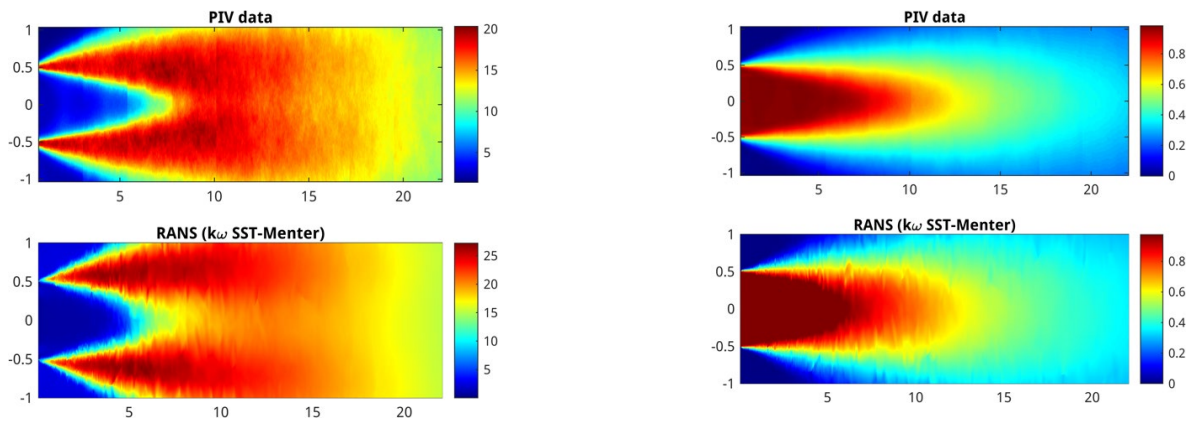


Figure 5. Comparison of turbulent kinetic energy (left) and axial velocity (right) contours with the experiment. Axis labels are x/D and y/D .

Unsteady Simulations

The next step was to compute the transient solution to characterize the shear layer instability behavior. An unsteady RANS with a second order finite difference (FD) temporal discretization, and a time step of 1.5×10^{-4} s to resolve up to Strouhal number 5.0 failed to generate any shear layer instability.

The failure of RANS to compute shear layer instability led to the use of a coarse LES on a modified computational domain discretized using the unstructured polyhedral FV grid (see Figure 6). Most of the FV cells in the previous mesh were required to resolve the boundary layers inside the nozzle, therefore, to reduce the computational expenditure the flow field 0.02 m ($x/D = 0.4651$) downstream of the nozzle was used as the inlet for the modified computational domain.

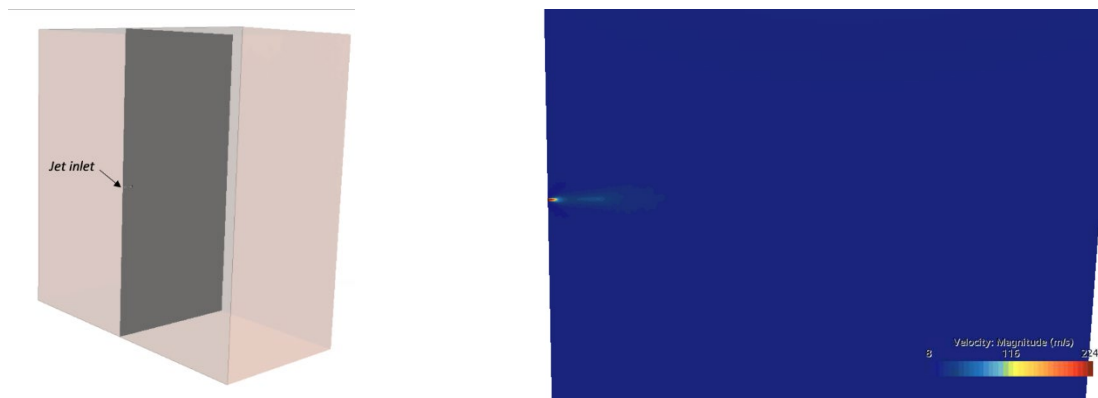


Figure 6. Computational domain of coarse large eddy simulations (LES) and initialized Reynolds-averaged Navier-Stokes (RANS) based solution.

The coarse LES domain was discretized with 3 million FV cells. The detail of the numerical scheme is given in below. Compared to the LES grid used in the fine grid simulations described in the last annual report, the selection of a cell size twice the original LES grid at the nozzle exit resulted in an unstructured mesh with 13 million cells. A bounded central scheme (second order with upwind blending factor of 0.15) with Roe inviscid flux was used for spatial discretization. The time step was 2.0×10^{-6} s with a second order temporal discretization. The wall-adapting local eddy viscosity (WALE) sub grid scale model ($C_w = 0.544$; $C_t = 3.5$; $\kappa = 0.41$) was implemented. For the fine grid LES, the spatial discretization used a trimmed mesh. The near wall resolution at the nozzle exit wall was 0.0004 m increasing to 0.024 m downstream of the



nozzle exit and then 0.001 m further downstream up to 0.42 m. This resulted in 42 million FV cells. The solution was initialized using steady state RANS, and then LES was implemented. A second order Central Difference scheme was used with turbulence modeled using the Dynamic Smagorinsky model with a filter width ratio of 2, and $C_t = 3.5$. A second order FD scheme discretized the temporal derivatives. Mach number contours for the fine grid LES are shown in Figure 7 for reference.

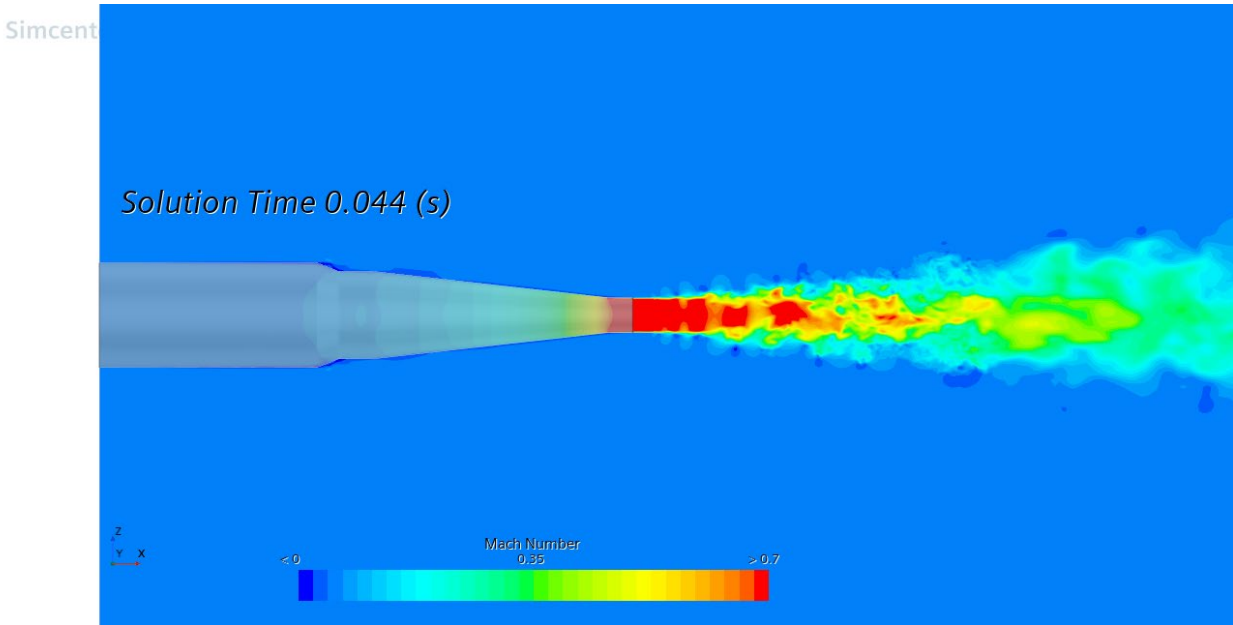


Figure 7. LES computation showing the Mach number contour.

Eigenfunction-based Forcing: Modal Analysis

Since coarse LES simulation failed to produce an unsteady behavior at the jet exit, eigenfunction-based small amplitude forcing at the inlet was used to generate shear layer instability in the coarse LES. A modal analysis of the shear layer profile using linear stability theory was performed 0.02 m downstream of the nozzle to include the low frequency modes. The velocity and temperature profiles were based on a hyperbolic tangent shape and fitted to the RANS-predicted profiles. These profiles of axial velocity, U and temperature, T are shown in Figure 8. The corresponding axial growth rates of the modes, based on linear stability theory (LST), are shown in Figure 9. The growth rate peaks at 2200 Hz, as shown in Figure 9. The corresponding mode shapes are shown in Figure 10.

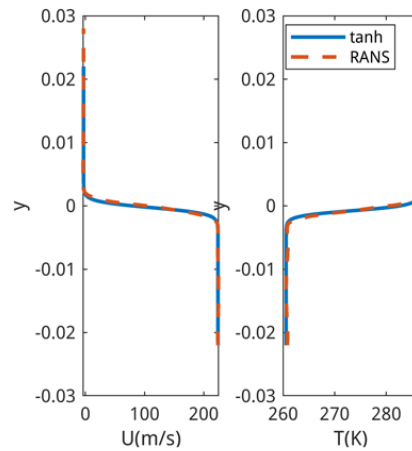


Figure 8. Comparison of hyperbolic tangent fit to the RANS simulations at 0.02 m downstream of the nozzle exit.



Figure 9. Growth rates of the shear layer instability from linear stability theory as a function of frequency and Strouhal number.

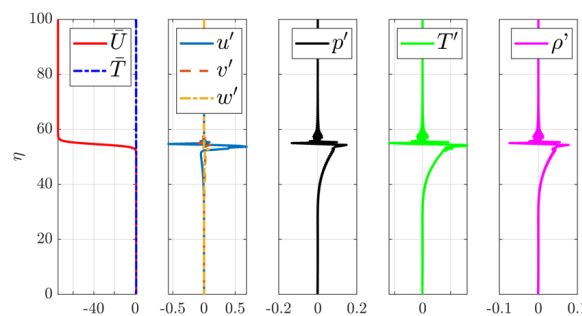


Figure 10. Kelvin-Helmholtz instability eigenfunctions computed from the linear stability analysis at 2200 Hz ($St = 0.4$) and axisymmetric mode.

The forcing at the jet exit was provided using a set of eigenfunctions at frequencies ranging from 500 to 3000 Hz with an interval of 500 Hz. The forcing set includes modes with angular wavenumbers varying from $\beta = 0$ to 2 with an interval of 0.25 for the same frequency range. Note that in this case, the spanwise wavenumber is approximated as angular wavenumber.



The forcing did result in unsteadiness in the jet's development, but not to the level of randomness seen in the fine LES simulations. This is seen in Figure 11 where the development of the forced jet (upper figure) is much slower than that of the unforced, fine LES case (lower figure).

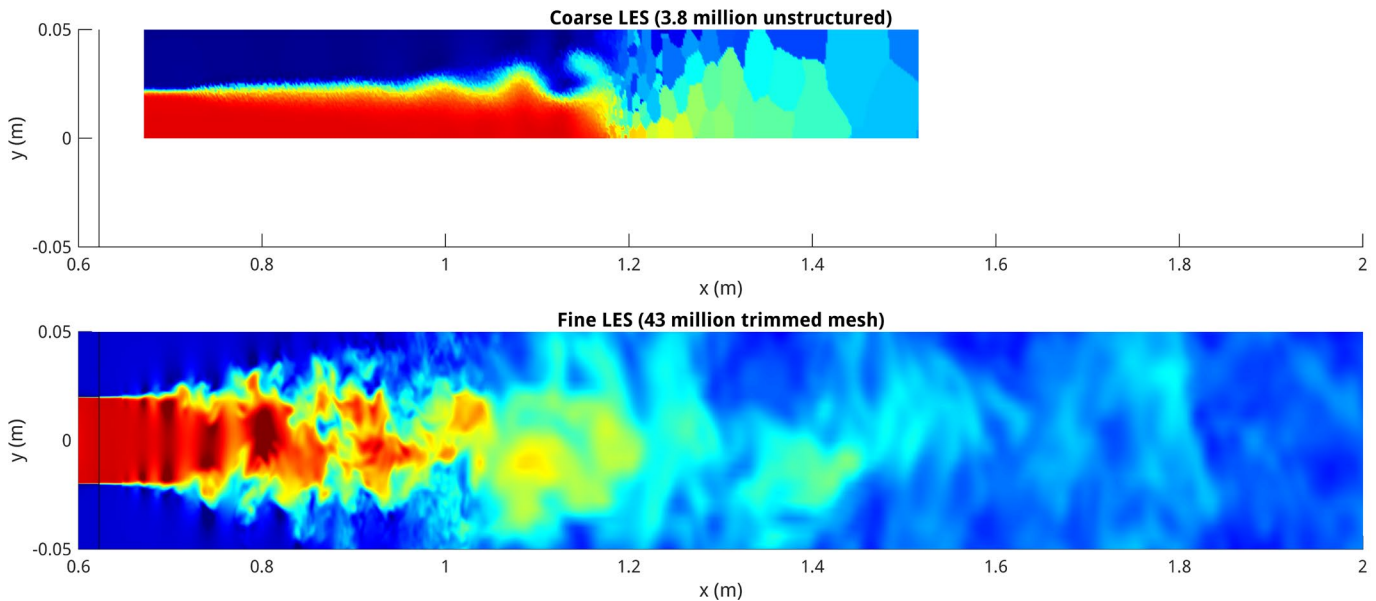


Figure 11. Comparison of initial jet development. Upper figure shows the excited jet case, and the lower figure shows the fine-grid LES simulation.

Task 2 - Hybrid RANS and LES Approach for Noise Efficient Predictions

Pennsylvania State University

Objective

The objective of this task is to develop a less computationally expensive approach. The basic concept and initial results were described in last year's annual ASCENT report. A summary and task progress are described below.

Research Approach

The idea arose from experimental results providing convincing evidence that jet noise consists of two characteristic source mechanisms. This was first proposed by Tam et al. (1996), who identified a small-scale similarity spectrum and a large-scale similarity spectrum. With these two spectral shapes, the radiated noise spectra of jets from a wide range of operating conditions could be matched very successfully. The original comparisons by Tam et al. (1996) were made for supersonic jets, but Viswanathan (2002) has shown that the same similarity spectra can be used to represent both subsonic and supersonic jet noise. A more recent overview of the "two-source model" has been given by Tam (2019). The two similarity spectra are shown in Figure 12.

Figure 13 shows how jet noise spectra at three polar angles can be decomposed into the two similarity spectra. At 90° , the full spectrum is described by the small-scale similarity spectrum. At 145° , both similarity spectra are required to match the full spectrum. Finally, at 165° , the large-scale similarity spectrum contributes almost completely to the full spectrum except for a possible contribution from the small-scale similarity spectrum at high Strouhal numbers. These examples are for an unheated $M_j = 0.51$ jet. For a higher Mach number, the large-scale similarity spectrum dominates over a wider-angle range. In addition, Tam and Zaman (2000) have shown that the same similarity spectrum can be used to represent the noise radiation to sideline directions for nozzles with tabs or rectangular nozzles, thus indicating that nozzle geometry has little influence on the noise radiation in these directions.

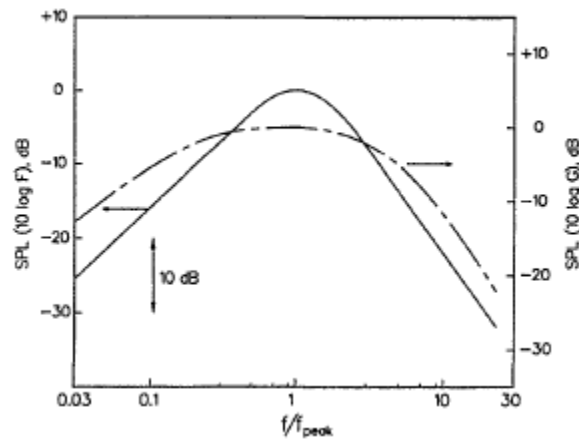


Figure 12. Similarity spectra for the two components of turbulent mixing noise. -----, large turbulent structures/instability wave noise; - - - - -, fine scale turbulence noise.

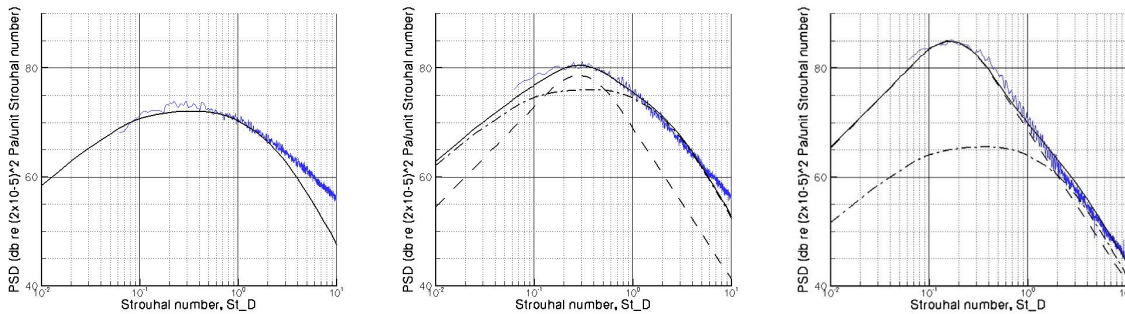


Figure 13. Demonstration of how the two similarity spectra can represent the full radiated noise spectrum at different polar angles: 90° (left), 145° (center), and 165° (right).

This behavior, particularly for the small-scale similarity spectrum, is similar to that displayed by the noise predictions using the Tam and Auriault (1999) prediction method for the noise from small-scale turbulence. Figure 13 shows predictions of jet noise from a convergent nozzle at the same acoustic Mach number of 0.875. One is unheated and has a static temperature ratio of 2.5.¹ The upper dataset is for the heated jet, and the lower set is for the unheated case. Predictions for three acoustic analogy models were performed by Gryazev et al. (2023). The models were those developed by Tam and Auriault (1999) and Khavaran and Bridges (2004), as well as the generalized acoustic analogy (GAA) by Goldstein and Leib (2008). The predictions for the Tam and Auriault model follow the trend seen in Figure 14, whereas the other models follow the experimental data more closely, because these models, particularly the GAA, attempt to model a non-isotropic source to represent noise radiation to large angles. The GAA model relies on LES to obtain the properties of the non-isotropic source, and whether the same properties would be retained if the geometry or complexity of the jet nozzle were different is unclear.

¹ These data were obtained as part of the Strategic Investment in Low-carbon Engine Tech program and were performed at QinetiQ.

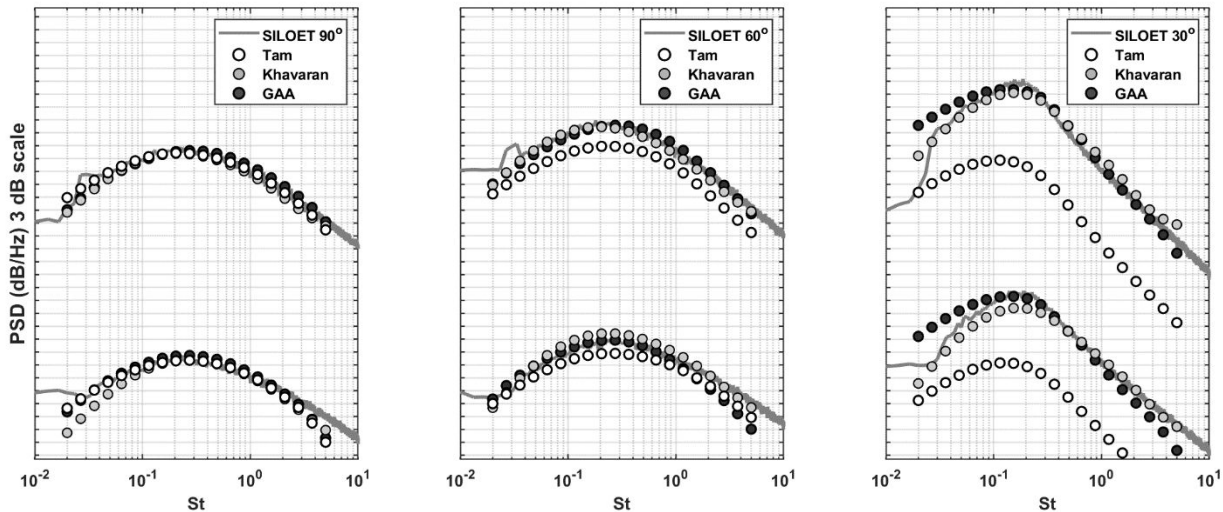


Figure 14. Noise spectra predictions of the cold (bottom) and hot (top) Strategic Investment in Low carbon Engine Technology (SILOET) jet, using the correlation scales based on the turbulent kinetic energy and dissipation rate reconstructed from RANS comparison.

These findings suggest that the Tam and Auriault (1999) model can represent the noise radiated by small-scale turbulence. The difference between the small-scale noise prediction and the full spectrum can be attributed to the contribution from the large-scale turbulence.

Due to time and personnel constraints no noise predictions using the acoustic analogy approach were completed. RANS predictions for several of the Georgia Tech experimental cases were performed as well as a RANS calculation for a rectangular jet; however, no noise predictions were made.

Awards

None.

Student Involvement

The Penn State team included one graduate research assistant, Dana Mikkelsen, who has been the lead on computational fluid dynamics simulations. During 2024, Dana Mikkelsen left Penn State to become a full-time employee of Gulfstream Aerospace. She graduated with Master of Science in Aerospace Engineering in December 2024. A senior graduate student, Mr. (now Dr.) Aravinth Sadagopan, provided computational support.

References

- Farassat, F., & Succi, G. P. (1982). The prediction of helicopter rotor discrete frequency noise. *American Helicopter Society*, 497-507. <https://api.semanticscholar.org/CorpusID:107210864>
- Ffowcs Williams, J., & Hawkings, D. L. (1969). Sound generation by turbulence and surfaces in arbitrary motion. *Philosophical Transactions for the Royal Society of London. Series A, Mathematical and Physical Sciences*, Goldstein, M. E., & Leib, S. J. (2008). The aeroacoustics of slowly diverging supersonic jets. *Journal of Fluid Mechanics*, 600, 291-337.
- Gryazev, V., Markesteijn, A. P., & Karabasov, S. A. (2023). Robustness of reduced-order jet noise models. *AIAA Journal*, 61(1), 315-328.
- Khavaran, A., & Bridges, J. (2004, May 10-12). *Modelling of turbulence generated noise in jets* [Conference paper]. 10th AIAA/CEAS Aeroacoustics Conference, Manchester, Great Britain. <https://doi.org/10.2514/6.2004-2983>
- Tam, C. K. (2019). A phenomenological approach to jet noise: the two-source model. *Philosophical Transactions of the Royal Society A*, 377(2159), 20190078.



- Tam, C. K., & Auriault, L. (1999). Jet mixing noise from fine-scale turbulence. *AIAA journal*, 37(2), 145-153.
- Tam, C., Golebiowski, M., & Seiner, J. (1996, May 6-8). *On the two components of turbulent mixing noise from supersonic jets* [Conference paper]. *Aeroacoustics conference*, State College, Pennsylvania. <https://doi.org/10.2514/6.1996-1716>
- Tam, C. K., & Zaman, K. B. M. Q. (2000). Subsonic jet noise from nonaxisymmetric and tabbed nozzles. *AIAA journal*, 38(4), 592-599.
- Viswanathan, K. (2002). Analysis of the two similarity components of turbulent mixing noise. *AIAA journal*, 40(9), 1735-1744.